

Permeable pavement hydraulic optimization by using an analytical-probabilistic model

Mariana Marchioni, Anita Raimondi ^{*}, Maria Gloria Di Chiano and Gianfranco Becciu

Department of Civil and Environmental Engineering (DICA), Politecnico di Milano, Piazza Leonardo da Vinci, 32, Milano 20133, Italy

*Corresponding author. E-mail: anita.raimondi@polimi.it

 AR, 0000-0003-1598-2265

ABSTRACT

On-source storage controls are a sustainable solution for stormwater management in a scenario of continuous urban area growth. Structures that manage storage volumes through infiltration include extra environmental benefits, such as groundwater recharge, evapotranspiration, and pollutant load removal. Permeable pavement systems are among these controls and can easily integrate into dense urban areas, resulting in paved surfaces contributing to stormwater management. The shift toward on-source strategies is encouraged through regulations, policies, incentives, and awareness campaigns, which are substantially increasing their dissemination. Optimizing the design of on-source storage controls with infiltration, such as permeable pavement systems, through robust methodologies can reduce reservoir depth, reducing environmental impact and costs without impact on reliability. The analytical-probabilistic (AP) method using derived probability distribution theory from rainfall event characteristics and the mathematical description of hydrologic processes within the permeable pavement systems provides an analytical equation that can be used as a design tool, proving robustness analogous with continuous simulations. Results obtained with the AP method were compared with traditional event-based methodologies and continuous simulation, assessing the reliability of the proposed method in optimizing permeable pavement systems' reservoir depth.

Key words: hydraulic design, permeable pavement systems, probabilistic methods of stormwater management, sustainable urban drainage

HIGHLIGHTS

- Permeable pavement systems are stormwater controls with temporary storage and infiltration, providing multiple benefits for the environment.
- This research proposes an analytical equation derived from probability distribution theory that can be used as a design tool for permeable pavement systems.
- The analytical probabilistic model was compared with event-based methods and continuous simulation.
- The analytical probabilistic model as a design tool provides reliability analogous to continuous simulations.

NOTATION LIST

μ	mean
b	rainfall interevent time
f	hydraulic conductivity
f_c	saturated hydraulic conductivity
h_{\max}	maximum water depth
I	inflow
IETD	minimum interevent time
N	concatenated storm events
N_{\max}	maximum managed storm events
P_R	probability of outflow (overflows and drain discharge if present)
R	outflow (sum of overflows and drain discharge if present)
r	ratio between contributing impervious surface and permeable pavement surface
S	pavement surface
SSE	sums of square error
T	return period

This is an Open Access article distributed under the terms of the Creative Commons Attribution Licence (CC BY 4.0), which permits copying, adaptation and redistribution, provided the original work is properly cited (<http://creativecommons.org/licenses/by/4.0/>).

u	rainfall event duration
v	rainfall event volume
W	water volume
W_{\max}	system storage capacity

ABBREVIATION LIST

AP	analytical-probabilistic model
PDF	probability density function
WB	water balance design method
WB24	water balance design method with 24 h storm
IDF	intensity duration frequency

1. INTRODUCTION

Conventional stormwater management typically relies on runoff conveyance, moving water down a basin and releasing it into watercourses, often without undergoing treatment. In a scenario of continuous urban population growth, leading to increased urban sprawl and subsequent land sealing, stormwater systems face a consistently rising challenge to manage larger runoff peak flow and volumes (Elliott & Trowsdale 2007; Woods-Ballard *et al.* 2007; Kim & Sansalone 2008; Sansalone *et al.* 2012; Goulden *et al.* 2018; UN DESA 2019). Stormwater strategies are shifting to encourage stormwater on-source controls through temporary storage and infiltration structures that also provide pollution load removal and additional potential ecosystem services benefits such as groundwater recharge, evapotranspiration increased, biodiversity, and amenities being called low impact development (LID), best management practices (BMPs), sustainable urban drainage systems (SuDS), and water sensitive urban design (WSUD) (Barbosa *et al.* 2012; Morgenroth *et al.* 2013; Nemirovsky *et al.* 2013; Brown & Borst 2015; Palla *et al.* 2015; Palla & Gnecco 2015; Marchioni & Becciu 2018; Altobelli *et al.* 2020; Brugin *et al.* 2020; Gobatti *et al.* 2022; Gobatti & Leite 2022; Langeveld *et al.* 2022). Such practices are often supported by local regulations and policies, incentives, and awareness campaigns (Dhakal & Chevalier 2017; Lieberherr & Green 2018). Permeable pavement systems are a control among those sustainable practices that allow using low-traffic paved areas such as parking lots to manage stormwater through infiltration and temporary storage, as well as load removal through filtration mechanisms (Sansalone *et al.* 2012; Marchioni & Becciu 2015; Winston *et al.* 2016, 2020; Lobo Marchioni *et al.* 2022). The system can be adapted in densely established urban contexts and fits a scenario of land sealing and mandatory implementation of stormwater controls by regulations and policies. Extensive research has been made to assess the system's performance confirming the efficiency in laboratory, full-scale tests and through modeling (Andersen *et al.* 1999; Brattebo & Booth 2003; Scholz & Grabowiecki 2007; Sansalone *et al.* 2012; Kuang & Fu 2013; Mullaney & Lucke 2014; Brown & Borst 2015; Lucke & Nichols 2015; Marchioni & Becciu 2015; Palla & Gnecco 2015; Andrés-Valeri *et al.* 2016, 2018; Coutinho *et al.* 2016; Kia *et al.* 2017, 2021; Turco *et al.* 2017, 2019, 2020; Brugin *et al.* 2020; Zhang & Chui 2020; Lobo Marchioni *et al.* 2021; Tirpak *et al.* 2021; Elizondo-Martínez *et al.* 2022). A typical permeable pavement system cross-section consists of a high-permeable surface, normally on pervious asphalt, pervious concrete, or interlocking concrete pavement, allowing prompt rainfall infiltration without generating runoff. The base is then normally filled with open-grade aggregates with a void content above 30%, providing stormwater temporary storage, allowing infiltration through the underlying soil, or slowly releasing the inflow through an underdrain pipe (Marchioni & Becciu 2015). Complementing the system, a geotextile is positioned above the subgrade, to protect the soil. If infiltration is not recommended by design constraints, i.e., underlying soil low permeability, expansive soil, contamination risk, an impermeable layer can be placed above the subgrade and the pavement behaves as a temporary storage control (Marchioni & Becciu 2015). Infiltration capacity reduction due to clogging can reduce the infiltration rate, although research shows that even under clogging conditions, permeable pavement systems can still reduce runoff and remove pollutants (Sansalone *et al.* 2012; Brown & Borst 2015; Kia *et al.* 2017; Razzaghmanesh & Borst 2018; Lobo Marchioni *et al.* 2021). Performance evaluation is held by estimating the hydraulic conductivity measurement, although the measurement is extremely dependent on the test method (Ranieri *et al.* 2012; Ravazzani *et al.* 2018; Feki *et al.* 2018, 2020; Lobo Marchioni *et al.* 2021).

The materials and construction stage account for 50% of costs and roughly 30% of greenhouse gas emissions and energy consumption on a permeable pavement, while specific reservoir layers account for less than 5% of

energy consumption and greenhouse gas emissions, where more than 90% of those impacts come from the surface layers (Liu *et al.* 2020; Chen & Wang 2022).

Permeable pavement systems' hydraulic design consists of sizing the permeable reservoir according to the maximum water depth (h_{\max}) and managing water inflow and outflow for a critical storm event. The h_{\max} must be enough to reduce outflows or ponding to an acceptable frequency of occurrence, represented by the return period (T) selected for the project. Usual event-based design methodologies consider the inflow of a single-storm event with a critical duration that yields the maximum storage volume required (Kia *et al.* 2021; Swan & Smith *s.d.*). By considering a single-storm event, these methodologies neglect the probability of storm events overlapping when the reservoir is not completely empty before the beginning of the next storm event. Initial soil saturation is also neglected and could lead to underestimation in certain cases (Abdalla *et al.* 2022). Critical rainfall duration is such that it yields h_{\max} and can be obtained analytically or by trial, considering various storm event durations. To further simplify design procedures, mainly for preliminary analysis, certain design method guidelines propose and/or establish a critical storm duration (Iqbal *et al.* 2022; Swan & Smith *s.d.*). For structures with infiltration, the outflow is obtained by considering hydraulic conductivity (f) constant and equal to the saturated hydraulic conductivity (f_c), neglecting the initial infiltration rate in unsaturated conditions, leading to an overestimation of h_{\max} (Riva *et al.* 2013; Feki *et al.* 2018, 2020; Ravazzani *et al.* 2018). Evaporation is usually neglected in favor of safety as it is generally small if compared to infiltration rates (Nemirovsky *et al.* 2013; Brown & Borst 2015). Hydraulic design methodologies also tend to neglect the rainfall-runoff transformation, slightly overestimating h_{\max} by neglecting the temporal dynamics of the kinematic wave (Riva *et al.* 2013). As reservoir excavation is a prominent factor in permeable pavement system costs, h_{\max} overestimation directly impacts costs, especially on large-scale projects. The design should therefore be adjusted by using continuous simulations to account for those uncertainties. Another possibility, however, would be using probabilistic models over design-storm methods, where the entire stochastic process of rainfall formation is considered. The analytical-probabilistic (AP) model, based on analytical models formulated with derived probability distribution theory, has been used to derive analytical equations describing various storm-water processes allowing the evaluation of the hydraulic performance on runoff volume, peak flow, water depth, and overflows for detention basins, water storage tanks, rain barrels, green roofs, rain gardens, and permeable pavement system for a chosen frequency of exceedance with robustness comparable with continuous long-term simulation with several application examples (Adams & Papa 2001; Bacchi *et al.* 2008; Raimondi & Becciu 2014a, 2014b, 2015; Becciu & Raimondi 2015; Yiping Guo *s.d.*; Zhang & Guo 2015a; Becciu *et al.* 2018; Raimondi *et al.* 2021; Guo *et al.* *s.d.*; Hassini & Guo 2022). The AP approach allows the selection of h_{\max} for a chosen frequency of exceedance and can be used as a design tool with the possibility to incorporate into the analytical equation the probability of the reservoir pre-filling from a previous storm event or to concatenate multiple storm events where the storage capacity is not completely available when a new storm event begins.

This research proposes the AP model as a design tool for a permeable pavement system, comparing the AP model results with conventional event-based methods and demonstrating their performance with a long-term continuous simulation using, as an example, rainfall data from São Paulo (Brazil), assessing the performance of the model on the Global South. The analytical equation proposed is derived from the permeable pavement hydraulic processes estimating the outflow probability for a given h_{\max} considering the probability of N concatenated events, that is, the probability of having a residual stored water volume from the $N - 1$ previous storm event. The AP approach has been previously used on permeable pavement systems, however, without considering the probability of concatenated events (Zhang & Guo 2015a; Guo *et al.* 2018).

2. METHODS

2.1. Hydraulic design methods

2.1.1. AP model

The AP model base assumption is that the main rainfall characteristics are independent and exponentially distributed, requiring the separation of a continuous rainfall series into independent storm events by adopting an adequate interevent time definition (IETD) (Adams & Papa 2001; Becciu *et al.* 2018; Guo *et al.* 2018). Then the permeable pavement's main hydrological processes are described with an analytical equation, and subsequently, this equation is derived based on the probability distribution theory.

Equation (1) represents the water balance (WB) for a permeable pavement system cross-section (Figure 1):

$$I = F + W + R \quad (1)$$

where I represents the inflow into the structure, R is the outflow, F is the infiltration on the underlying soil, and W is the stored rainwater volume. If the system is provided with an underdrain, the outflow R is the sum of the overflow volume and drain discharge; for a permeable pavement system without underdrains, R is the volume of overflow as ponding. Stormwater stored in the permeable pavement reservoir can range from zero to W_{\max} , representing the system storage capacity. For a permeable pavement system without underdrains, the storage capacity W_{\max} is represented by the void space on the reservoir layer.

The storage capacity from depression storage is neglected, and the void space available on the surface layer is not considered for temporary storage to avoid damaging the surface structure (Elizondo-Martinez *et al.* 2020).

Inflow toward the permeable pavement system includes runoff from contributing impervious areas ($r \cdot S$) and rainwater directly falling onto the pavement surface (S) (Equation (2)):

$$I = S + r \cdot S \quad (2)$$

r is the ratio between the contributing impervious surface and the permeable pavement surface.

The surface infiltration capacity and gravel aggregate layer have been assumed to be always greater than the inflow rate into the system. Only in cases where the surface is completely clogged does the infiltration capacity fall below the inflow rate, requiring maintenance procedures. Initial abstractions due to depression storage are neglected in Equations (1) and (2), which are excluded directly from the rainfall series.

In a functional permeable pavement, overflows as ponding should be avoided (full underlying soil infiltration) or, if underdrains are present, limited to downstream network capacity or discharge limitations imposed by regulations. The outflow probability is estimated by considering the water content in the system at the end of a generic storm event:

$$W_i = \begin{cases} W_{i-1} - f \cdot b_i + I_i - f \cdot u_i & \text{Condition}_1 \\ I_i - f \cdot u_i & \text{Condition}_2 \\ W_{\max} & \text{Condition}_3; \text{Condition}_4 \\ 0 & \text{Otherwise} \end{cases} \quad (3)$$

*Condition*₁: $W_{i-1} - f \cdot b_i > 0$; $0 < W_{i-1} - f \cdot b_i + I_i - f \cdot u_i < W_{\max}$

*Condition*₂: $W_{i-1} - f \cdot b_i \leq 0$; $0 < I_i - f \cdot u_i < W_{\max}$

*Condition*₃: $W_{i-1} - f \cdot b_i \leq 0$; $I_i - f \cdot u_i \geq W_{\max}$

*Condition*₄: $W_{i-1} - f \cdot b_i > 0$; $W_{i-1} - f \cdot b_i + I_i - f \cdot u_i \geq W_{\max}$

for $i = 1, \dots, N$ where N is the number of considered rainfall events.



Figure 1 | Permeable pavement system typical cross-section with a permeable concrete surface, permeable reservoir with open-graded coarse aggregates, and underdrains.

b represents rainfall IET and u rainfall represents event duration. Variable f in equations represents hydraulic conductivity, assumed constant and equal to the underlying soil-saturated hydraulic conductivity.

Water content for initial conditions, W_0 , ($i = 0$) results:

$$W_0 = \begin{cases} I_0 - f \cdot u_0 & 0 < I_0 - f \cdot u_0 < W_{\max} \\ W_{\max} & I_0 - f \cdot u_0 \geq W_{\max} \\ 0 & I_0 - f \cdot u_0 \leq 0 \end{cases} \quad (4)$$

Considering Equation (3): *Condition*₁ expresses the case of pre-filling from a previous storm event at the end of the considered event and this does not produce runoff; *Condition*₂ expresses the case where there is no pre-filling from previous storm events at the end of the considered event and does not generate runoff; *Condition*₃ expresses the case there is no pre-filling from previous rainfall event at the end of the considered event and generates runoff; *Condition*₄ expresses the case of pre-filling from previous rainfall event at the end of the considered event and this generates runoff.

Overflow from a permeable pavement system is a random variable, strictly depending on rainfall characteristics, the infiltration rate of the underlying soil, and the maximum storage capacity of the system, resulting in:

$$R_i = \begin{cases} W_{i-1} - f \cdot b_i + I_i - f \cdot u_i - W_{\max} & \text{Condition}_1 \\ I_i - f \cdot u_i - W_{\max} & \text{Condition}_2; \text{Condition}_3 \\ W_{\max} - f \cdot b_i + I_i - f \cdot u_i - W_{\max} & \text{Condition}_4 \\ 0 & \text{Otherwise} \end{cases} \quad (5)$$

Considering Equation (5):

*Condition*₁: $W_{i-1} < W_{\max}$; $W_{i-1} > f \cdot b_i$; $W_{i-1} - f \cdot b_i + I_i - f \cdot u_i > W_{\max}$

*Condition*₂: $W_{i-1} < W_{\max}$; $W_{i-1} \leq f \cdot b_i$; $I_i - f \cdot u_i > W_{\max}$

*Condition*₃: $W_{i-1} \geq W_{\max}$; $W_{\max} \leq f \cdot b_i$; $I_i - f \cdot u_i > W_{\max}$

*Condition*₄: $W_{i-1} \geq W_{\max}$; $W_{\max} > f \cdot b_i$; $W_{\max} - f \cdot b_i + I_i - f \cdot u_i > W_{\max}$

for $i = 1, \dots, N$ where N is the number of considered rainfall events.

Outflow for $i = 0$, R_0 results:

$$R_0 = \begin{cases} I_0 - f \cdot b_0 - W_{\max} & I_0 - f \cdot b_0 > W_{\max} \\ 0 & \text{Otherwise} \end{cases} \quad (6)$$

with reference to Equation (5): *Condition*₁ expresses the case there is no outflow at the event $i - 1$, there is pre-filling from the event $i - 1$ at the beginning of the event i and there is runoff from the permeable pavement at the end of the event i ; *Condition*₂ expresses the case there is no outflow from event $i - 1$, there is no pre-filling from event $i - 1$ at the beginning of event i and there is runoff from the permeable pavement at the end of event i ; *Condition*₃ expresses the case that there is outflow from event $i - 1$, there is no pre-filling from event $i - 1$ at the beginning of event i and there is runoff from the permeable pavement at the end of event i ; *Condition*₄ expresses the case there is outflow from event $i - 1$, there is pre-filling from event $i - 1$ at the beginning of event i and there is runoff from the permeable pavement at the end of event i .

h_{\max} can be obtained with the following equation considering the porosity of the reservoir filling material:

$$h_{\max} = \frac{W_{\max}}{p} \quad (7)$$

An AP model has been proposed to design the reservoir depth for a certain probability of outflows. The method is based on the derivation of the probability distribution functions (PDFs) of the variable of interest from the PDFs of the input variables, in this case, the rainfall series' main characteristics, and the mathematical representations of the hydrologic processes occurring in the permeable pavement. Also, the model considers input rainfall variables, namely rainfall depth, rainfall duration, and IET, as independent and exponentially distributed. To proceed with the application of the AP model, it is necessary to isolate the rainfall-independent storm events from the

recorded continuous rainfall time series. Rainfall statistics vary depending on how the events are delimited (Chin *et al.* 2016; Molina-Sanchis *et al.* 2016). Several approaches have been proposed for the identification of rainfall events; for example, Ignaccolo & De Michele (2010) proposed a definition of a rain event based on the statistical properties of inter-drop time intervals. A common criterion used by hydrologists to identify isolated rainfall events is the minimum IET, which consists of the minimum dry period between rainfall occurrences that characterizes them as independent (Dunkerley 2008; Barbosa *et al.* 2012; Freitas *et al.* 2020; Brasil *et al.* 2022; Cao *et al.* 2023). If the IET between two consecutive rainfall events is lower than IETD, the two storms are joined in a single event; otherwise, they are considered independent. In the literature, different methods to select IETD have been proposed. Medina-Cobo *et al.* (2016) used a multifractal characterization of rainfall for this purpose. Lee & Kim (2018) proposed the determination of IETD using an exponential function. Traditional techniques for the determination of IETD include autocorrelation analysis, the coefficient of variation analysis, and the mean annual number of rainfall events analysis. The autocorrelation coefficient method consists of choosing the values for which the coefficient of variation tends to be one. The coefficient of variation analysis is based on the theory that the probability density of IET for rainfall time series is like the exponential distribution. The coefficient of variance analysis is a method to determine IETD when the mean of IET is the same as the standard deviation of IET. For the third methodology, based on the mean annual number of rainfall events, IETD is the value of IET where the mean annual number of rainfall events becomes constant as IET increases. In practice, IETD must be related to catchment response characteristics; generally, shorter IETD is suggested for small urban catchments with quick concentration times, while for large rural catchments, IETD can also be several hours.

Different studies highlighted that exponential PDF provides a good fit to frequency histograms of main rainfall characteristics (Eagleson 1978; Adams *et al.* 1986; Bacchi *et al.* 2008; Bedient *et al.* 2008). Becciu & Raimondi (2012) observed better goodness for the double-exponential using rainfall data from Milan; however, the complexity of the expressions derived by the integration, without consistently improving the robustness of the results, ended up leading them to adopt the exponential probability density function (PDF). Table 1 gathers the PDFs and distribution parameters for the main rainfall characteristics.

Considering the derived probability distribution theory, the outflow probability can be estimated from the derived PDFs from rainfall depth v , rainfall duration u , and IET b (Benjamin & Cornell 1970). Considering $v = v_i = v_{i+1}$, $u = u_i = u_{i+1}$, $b = b_i = b_{i+1}$ in Equation (9); leads to exclude *Condition*₂.

Outflow probability has been estimated, distinguishing two different conditions: when the maximum emptying time, i.e., the time to completely drain the storage volume, is larger or smaller than IETD. For Case 1, the pre-filling from previous storm events at the beginning of the considered event is not considered, whereas for Case 2, the probability of a reduction in storage capacity due to a previous storm event is considered. A threshold outflow volume \bar{R} was considered related to discharge under the drainage network constraints. The outflow probability for cases 1 and 2 is obtained with the following equations, respectively.

Case 1: $W_{\max}/f \leq \text{IETD}$:

$$P_R = P(R > \bar{R}) = \int_{v=\frac{W_{\max} + \bar{R} + f \cdot u}{1+r}}^{\infty} p_v \cdot dv \int_{u=0}^{\infty} p_u \cdot du = \gamma \cdot e^{-\frac{\xi}{1+r} \cdot (W_{\max} + \bar{R})} \quad (8)$$

$$\text{with } \gamma = \frac{\lambda \cdot (1+r)}{f \cdot \xi + \lambda \cdot (1+r)}$$

Table 1 | Probability density functions of rainfall characteristics

Rainfall characteristic	Exponential PDF	Distribution parameter
Rainfall event volume (v ; mm)	$f(v) = \xi \cdot e^{-\xi \cdot v}$	$\xi = 1/\mu_v$
Rainfall event duration (u ; h)	$f(u) = \lambda \cdot e^{-\lambda \cdot u}$	$\lambda = 1/\mu_u$
Rainfall interevent time (b ; h)	$f(b) = \psi \cdot e^{-\psi \cdot (b - \text{IETD})}$	$\psi = 1/(\mu_b - \text{IETD})$

Case 2: $W_{\max}/f > \text{IETD}$:

$$\begin{aligned}
 P_R = P(R > \bar{R}) &= \int_{u=0}^{\infty} p_u \cdot du \int_{v=\frac{W_{\max} + \bar{R} + f \cdot u}{1+r}}^{\infty} \\
 &= P_R = \gamma \cdot \left\{ e^{-\frac{\xi}{1+r} \cdot (W_{\max} + \bar{R})} - \psi \cdot (1+r) \cdot \sum_{i=2}^N \left[(i-1) \cdot \beta_i \cdot e^{-\frac{\xi}{(1+r) \cdot (i-1)} \cdot [f \cdot \text{IETD} \cdot (i-2) + w_{\max}]} \right. \right. \\
 &\quad \left. \left. + i \cdot \beta_i^* \cdot e^{-\frac{\xi}{i \cdot (1+r)} \cdot [\bar{R} + W_{\max} + f \cdot \text{IETD}(i-1)]} \cdot \xi \cdot f \cdot \beta_i \cdot \beta_i^* \cdot e^{\psi \cdot \text{IETD} + \frac{\psi}{f} \cdot [\bar{R} \cdot (i-1) - w_{\max}]} \right. \right. \\
 &\quad \left. \left. - \frac{\xi}{1+r} \cdot (2 \cdot \bar{R} + w_{\max} - i \cdot \bar{R}) \right\} \right\} \tag{9}
 \end{aligned}$$

where $\beta_i = \frac{1}{\xi \cdot f \cdot (i-2) + \psi \cdot (i-1) \cdot (1+r)}$; $\beta_i^* = -\frac{1}{i \cdot \psi \cdot (1+r) + (i-1) \cdot \xi \cdot f}$

2.1.2. Event-based, WB for a 24-h storm event (WB24)

This design method is event-based representing the hydraulic processes on the permeable pavement operation with the inflow from a 24-h storm event from the permeable pavement and contribution areas and the outflow as the soil-saturated hydraulic conductivity within an estimated storage filling time (Equation (10)):

$$h_{\max} = \frac{H \cdot r + H - f_c t}{p} \tag{10}$$

where H is the rainfall depth, recommended using a 24-h storm event; f_c is the saturated hydraulic conductivity; t is the storage filling time, recommended 2 h; p is the porosity of the reservoir filling material.

The method neglects evapotranspiration and the initial infiltration rate of the underlying soil, adopting a constant hydraulic conductivity under saturation conditions (f_c). The inflow resulting from precipitation reaches the permeable pavement instantly, a hypothesis reasonable since water falling on the pavement takes a few seconds to reach the bottom of the pavement due to the high permeability of the surface and reservoir layers. Initial abstractions due to depression storage and the initial wetting of the surface and reservoir materials are not considered. This method does not consider the identification of a critical storm event but recommends adopting a 24-h storm event, tendentially overestimating the results.

2.1.3. Event-based WB

The event-based WB method also describes the hydrological processes of a permeable pavement system for a single-storm event. The water volume stored in the reservoir can be represented by the WB (Equation (11)):

$$(Q_e - Q_u) \cdot dt = dW \tag{11}$$

where Q_e is the inflow; Q_u is the outflow; ΔW is the variation of volume storage in the permeable pavement reservoir; Δt is the time interval.

The inflow, Q_e , is a function of the rainfall duration (u) and can be obtained with the following equation:

$$Q_e = \varphi \cdot A \cdot a \cdot u^{n-1} \tag{12}$$

where a and n are the parameters of the binomial intensity duration frequency curve; A is the total contribution area (permeable pavement area plus eventual contribution areas); φ is the runoff coefficient.

The outflow, Q_u , is obtained considering the f_c from the underlying soil, as in the following equation:

$$Q_u = f_c \cdot A_p \quad (13)$$

where f_c is the saturated hydraulic conditions and A_p is the permeable pavement area.

The storage volume in function of time can be obtained by the following equation:

$$W(t) = p \cdot A_p \cdot h(u) \quad (14)$$

where $h(t)$ is the water depth as a function of storm duration; p is the porosity of the reservoir filling material.

By inserting Equations (12)–(14) into Equation (11), it is possible to obtain the water depth as a function of storm duration:

$$h(u) = \frac{u}{p} \cdot (\varphi \cdot a \cdot u^{n-1} \cdot R - f_c) \quad (15)$$

The maximum water depth, h_{\max} , is then obtained with Equation (17) using the critical storm duration, u_w . The u_w is obtained by deriving Equation (15) for u and equaling zero (Equation 16):

$$\frac{dh}{du} = \varphi \cdot a \cdot n \cdot R \cdot \frac{u^{n-1}}{p} - \frac{f_c}{p} = 0 \quad (16)$$

$$u_w = \left(\frac{f_c}{\varphi \cdot a \cdot n \cdot R} \right)^{\frac{1}{n-1}} \quad (17)$$

Thus, h_{\max} can be obtained with Equation (18) after obtaining u_w with Equation (17).

$$h_{\max} = h(u_w) = \frac{u_w}{p} \cdot (\varphi \cdot a \cdot u_w^{n-1} \cdot R - f_c) \quad (18)$$

This method also neglects evapotranspiration, the initial infiltration rate of the underlying soil, and rainfall-runoff transformation.

2.2. Application of design methods

The AP approach was applied to a case study using rainfall data from São Paulo (Brazil) and then compared with the event-based methods (WB and WB24). According to the Köppen classification, Sao Paulo has predominantly a Cfa climate (humid subtropical climate) with a mean annual precipitation of 1,356 mm and a temperature of 20.6 °C (Alvares *et al.* 2013; Beck *et al.* 2018). São Paulo has typical sandy loamy soil (SM, SC from Soil-USCS), with f_c ranging from 10^{-9} to 10^{-6} m/s. The following f_c were used for all design methods and the continuous simulation: 3.6, 1.8, and 0.36 mm/h.

The event-based methods (WB and WB24) used the intensity duration frequency (IDF) equation for São Paulo Station IAG/USP – E3-035 (23° 39' 04" 46° 37' 21") (Equation (19)) with return periods of $T = 2, 5, 10, 20, 50,$ and 100:

$$i(u, T) = 39.3015 (u + 20)^{-0.9228} + 10.1767 (u + 20)^{-0.8764} \cdot \left[-0.4653 - 0.8407 \ln \ln \left(\frac{T}{T-1} \right) \right] \quad (19)$$

where i is the rainfall intensity; u is the rainfall duration; T is the return period.

The flowchart in Figure 2 describes the steps for using the AP approach, starting from the rainfall time series. The rainfall parameters required to use the AP method were obtained from a rainfall data set recorded at Station ID 273 in São Paulo (Brazil) from 2007 to 2017 with a 10-min interval time supplied by FCTH (Fundação Centro Tecnológico de Hidráulica). The number of concatenated storm events (N) was adjusted to give the best fit between the continuous simulation of the hydraulic-hydrologic processes (Equations (5) and (6)) and the

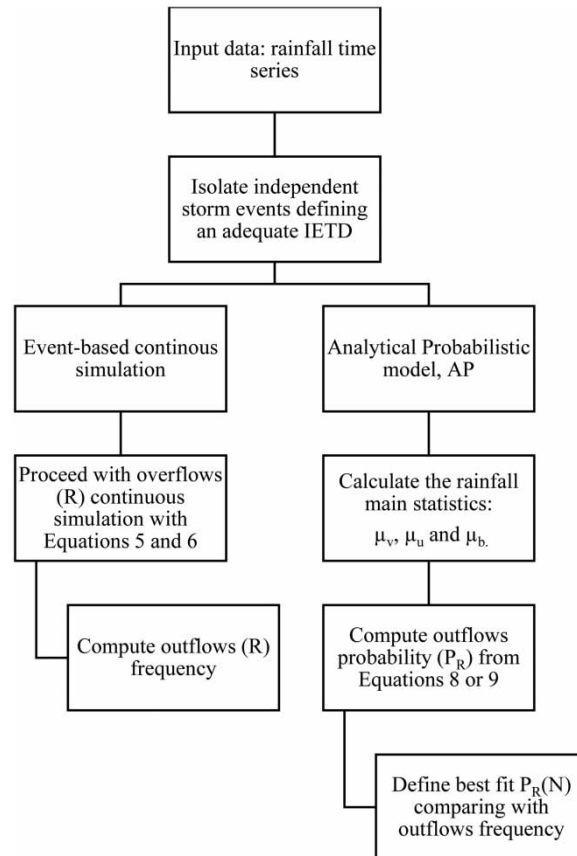


Figure 2 | Flowchart for the AP approach from the rainfall time series.

analytical equation (Equations (8) and (9)) evaluating the sums of square error (SSE). The contribution areas $r = 0, 1, 2,$ and 5 were considered.

A continuous simulation for the same rainfall series was held using the Environmental Protection Agency Storm Water Management Model (EPA-SWMM). The model considers evapotranspiration but neglects the initial infiltration rate; using a constant seepage value equals the f_c of the underlying soil (Zhang & Guo 2015b; Xu *et al.* 2017; Randall *et al.* 2020; Abdalla *et al.* 2021). The permeable pavement was simulated as a LID occupying the entire catchment, with the main characteristics as shown in Table 2.

The pavement cross-sections for EPA-SWMM simulations included an underdrain with an offset distance equal to h_{\max} , where discharge would start when the water depth reaches h_{\max} . The total depth of the reservoir was considered h_{\max} plus the diameter of the underdrain, in this case, 100 mm. Different h_{\max} were used from a depth $h_{\max} = 0$ mm, where the reservoir depth would be equal to 100 mm, to a depth $h_{\max} = 600$ mm. A 10-min time step was used for rainfall-runoff and routing modeling during wet periods, and a 60-min time step for dry periods. R_{SWMM} represents the frequency of outflows through the underdrains and was obtained considering the total events with outflows by the total storm events, in this case with IETD being the Δt of the rainfall series ($\Delta t = 10$ min).

3. RESULTS AND DISCUSSION

3.1. AP model

The application of the AP required the selection of an IETD, resulting in independent, exponentially distributed storm events. Table 3 shows the coefficient of variation (CV) for IETD from 1 to 12 h for the São Paulo rainfall data set, considering initial abstraction equal to 2 mm, where the IETD of 4 h was selected for the application of the AP approach. Selecting the appropriate IETD can assure that the discrete storm events are statistically independent (Adams & Papa 2001). The assumption of exponential distributions fits well for rainfall depth (v) and duration (u) but less for IET (b), similar results were obtained from previous research with rainfall data from

Table 2 | Permeable pavement main characteristics used for the EPA-SWMM simulation

Description	Value
Pavement thickness (mm)	80
Void ratio (void/solids)	0.15
Permeability (mm/h)	300
Surface roughness (Manning n)	0.1
Surface slope (per cent)	1
Storage void ratio (void/solids)	0.4

Table 3 | Coefficient of variation, CV for IETD from 1 to 12 h

IETD	CV_v	CV_u	CV_b
1	1.05	1.12	0.53
2	1.03	1.08	0.56
3	1.01	1.03	0.58
4	0.99	1.02	0.60
5	1.00	0.94	0.61
6	1.00	0.93	0.63
12	1.10	0.91	0.69

Note: Bold indicates the IETD selected for the analytical-probabilistic approach.

Milan, humid subtropical climate (Beck *et al.* 2018) and rainfall time series (Becciu & Raimondi 2012; Raimondi & Becciu 2014a, 2014b; Raimondi *et al.* 2022, 2023; Di Chiano *et al.* 2023). Table 4 gathers the main statistical parameters for the rainfall characteristics of the independent rainfall events for the 4-h IETD and Figure 3 plots the PDF for the rainfall characteristics for the 4-h IETD.

The Pearson correlation coefficient for the considered hydrological parameters is gathered in Table 5, where rainfall event volume and event duration are weakly correlated, while rainfall event volume and IET and rainfall event duration and IET are very weakly correlated.

The AP approach proposed an analytical equation (Equations (8) and (9)) that gives the expected value of outflows, in this case, overflows (without underdrains) in a permeable pavement for a certain h_{\max} from the statistical representation of the rainfall data, considering the probability of concatenate storm events. The following contribution areas from $r = 0, 1, 2,$ and 5 were considered, with the exception of $f_c = 0.36$ mm/h, where $r = 5$ yields h_{\max} over 5 m and was not considered. The frequency of outflows was obtained considering the representation of the hydraulic processes (Equations (5) and (6)) with outflows observed after each storm event and the total observed events.

Figure 4 gathers the outflow frequency (Equations (5) and (6)) and probability with the AP approach (Equations (8) and (9)). The number of concatenated storm events was defined considering the best fit between frequency and probability using SSE. By reducing f_c , the influence of concatenate events increases as draining time also increases, and so does the probability that the permeable pavement reservoir is not empty before a new storm event. Table 6 shows the goodness of fit and the number of concatenated events for the considered cases.

Table 4 | Main statistical parameters for rainfall characteristics for IETD = 4 h

	Rainfall depth, v (mm)	Rainfall duration, u (h)	Rainfall interevent time, b (h)
Mean, μ	14.80	8.57	91.96
Standard deviation, S	14.68	8.38	152.68
Variation coefficient, CV	0.99	1.02	0.60

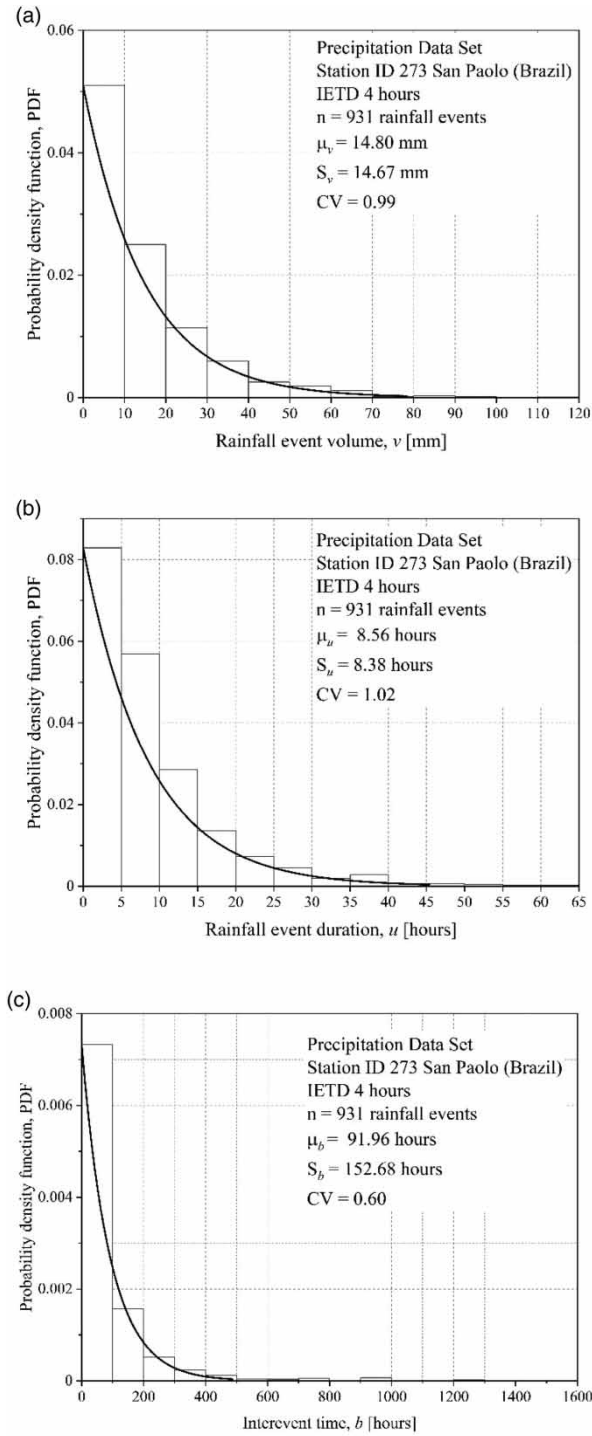


Figure 3 | Histogram and PDF for precipitation data set from Station ID 273 in São Paulo (Brazil) from 2007 to 2017 with a 10-min interval time and IETD of 4 h. (a) Rainfall event volume (v), (b) rainfall event duration (u), and (c) interevent time (b).

Table 5 | Pearson correlation coefficient for precipitation data set main parameters

$\rho_{v,u}$	0.418
$\rho_{v,b}$	-0.06
$\rho_{u,b}$	-0.02

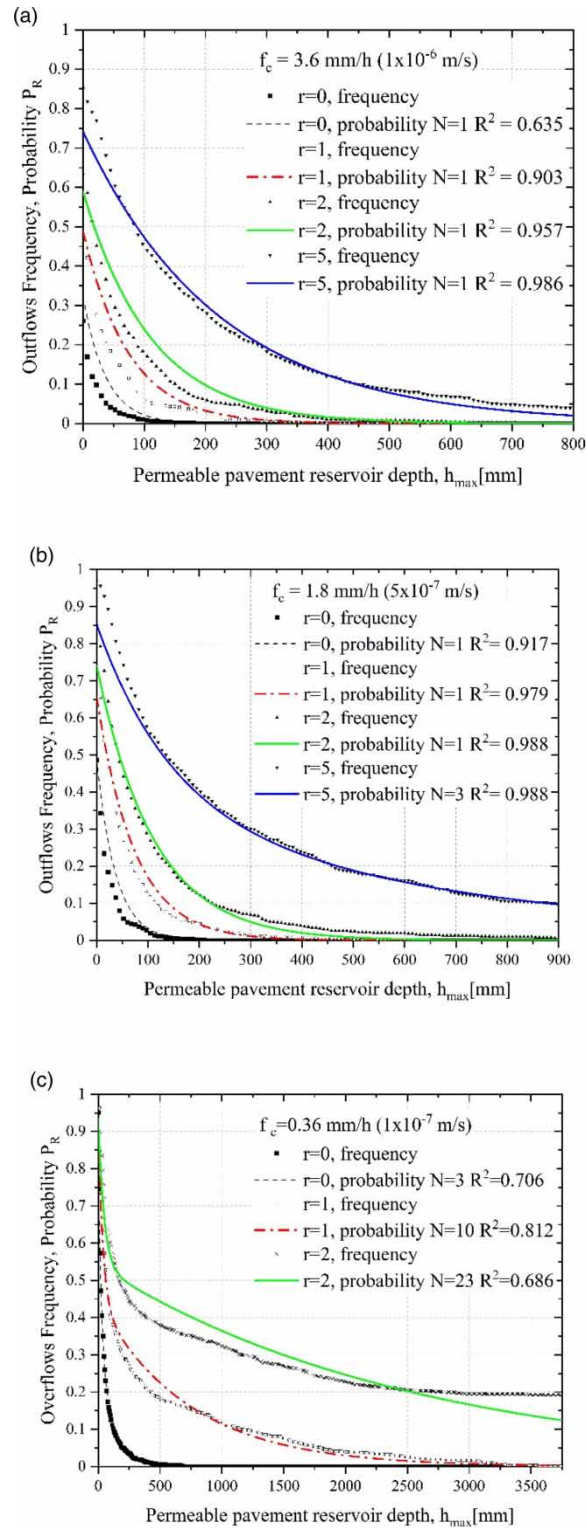


Figure 4 | Outflows frequency and probability with the analytical equation from the probabilistic model for contribution area equals $r = 0, 1, 2,$ and 5 . N represents the number of concatenate events with the best fit evaluated using R -squared. (a) Soil-saturated hydraulic conductivity, $f_c = 3.6 \text{ mm/h}$ ($1 \times 10^{-6} \text{ m/s}$); (b) soil-saturated hydraulic conductivity, $f_c = 1.8 \text{ mm/h}$ ($5 \times 10^{-7} \text{ m/s}$); (c) soil-saturated hydraulic conductivity $f_c = 0.36 \text{ mm/h}$ ($1 \times 10^{-7} \text{ m/s}$).

Observing Figure 4 for $f_c = 3.6 \text{ mm/h}$, it is noticed that for small h_{max} , there is an underestimation of the probability of outflow, and as h_{max} increases, the probability of outflows tends to be overestimated by the AP. For the $f_c = 1.8 \text{ mm/h}$, there is a better goodness of fit between frequency and probability overall, with r -squared above

Table 6 | Goodness of fit for outflow frequency and probability with analytical equation for the AP approach

Hydraulic conductivity, f_c (mm/h)	Contribution area ratio, r (-)	Number of concatenated events, N	R^2
3.6	0	1	0.635
	1	1	0.903
	2	1	0.957
	5	1	0.86
1.8	0	1	0.917
	1	1	0.979
	2	1	0.988
	5	3	0.988
0.36	0	3	0.706
	1	10	0.812
	2	23	0.686

0.80 for all contribution areas considered. Outflow probability was underestimated in both extremes. For $f_c = 0.36$ mm/h, classified as a low permeability in soil classification (Terzaghi *et al.* 1996), for $r = 2$, the outflow frequency was underestimated for h_{\max} above 2,500 mm with a trend contrary to the previous cases, while for $r = 1$, above $h_{\max} = 1,000$ mm, the probability was slightly underestimated. For $h_{\max} = 200$ mm, the probability was, however, slightly overestimated. The analytical equation gives the best fit when the inflow (permeable pavement area + contribution area) and outflow (soil infiltration represented by the hydraulic conductivity) are not excessively diverse. Within the limits normally used for stormwater controls on the probability of outflow ($T =$ five years, $P = 0.2$), the AP overestimates the h_{\max} . As the soil permeability decreases, the low release of the storage volume increases the probability of overlapping storm events, and to take account of that N increases. For the present application, N was set by comparing it with the event-based continuous simulation, but to be easily adopted as a design tool, the AP would require defining N without a recorded rainfall time series. N is a function of both f_c and rainfall characteristics, where the available time to completely drain a storm event with depth v is a function of the sum of duration u and IET b and the soil hydraulic conductivity. The number of concatenated events could be suggested by comparing the inflow and outflow.

The AP I is a process-oriented model with input on field measurement data (f_c , rainfall characteristics), a parameter N that is a function of local conditions, and a design variable (W_{\max} , h_{\max}). The output is the probability of outflow (P_R) considering the constraint of the R threshold. Model uncertainties are first linked to field measurements, both on f_c and rainfall recorded data. The measurement of the underlying soil f_c is highly dependent on the test method and soil conditions and can decrease over time due to clogging and the effects of soil compaction (Ranieri *et al.* 2012; Feki *et al.* 2018, 2020). As f_c decreases, to maintain P_R h_{\max} increases, where a 90% reduction in f_c increases by 200% in h_{\max} to maintain the same P_R . Rainfall data are also subject to measurement errors, where recorded series from nearby stations are normally used for adjustments (Di Chiano *et al.* 2023). Isolating the continuous series on independent exponentially distributed storm events by selecting an IETD plays a crucial role in determining the model's outcome and can lead to a variation of 60% on P_R .

For this example, the parameter N was selected by identifying the least SSE between outflow frequency and P_R . In cases where $N > 1$, increasing N initially increases goodness until an optimal N is reached. For example, for $f_c = 1.8$ mm/h, the best fit between outflow frequency and P_R was reached with $N = 3$ (SSE = 0.12) with SSE ranging from 1.34 ($N = 1$) to 8.60 ($N = 50$). As N increases, P_R increases on a logarithmic scale, eventually reaching a stable value.

3.2. Comparison of design-storm, probabilistic approach methods, and continuous simulation

Both WP24 (Equation (10)) and WP (Equation (18)) considered a single-storm event from an IDF equation with a critical duration. WP24 establishes a 24-h storm event while WP searches for the critical storm event, considering inflow and outflow. For an exponential distribution of storm duration and depth this constraint is reasonable as for low-permeability soil the critical storm tends to result in a 24-h duration or higher. For high-permeable soils, the critical storm could have short durations, but the high permeability would drain the reservoir promptly after the end of the storm event. The WB method required binomial IDF parameters, obtained by regression and mean squared error from Equation (19). Both methods neglect storage pre-filling and the effect of overlapping storm

events and consider a certain frequency (return period) of events. The AP model used as a design tool gives the outflow probability (P_R) for a chosen h_{\max} , while the WB24 and WB obtained a h_{\max} for a frequency represented by the return period on the IDF equation, which can also be translated as an outflow probability (Guo & Adams 1999).

Table 7 and Figure 5 gather P_R , T , and h_{\max} obtained with the three methods (WB24, WB, and AP). There is a clear h_{\max} overestimation for WB24 followed by the WB. The AP design method led to an overall h_{\max} of 69% smaller when compared with the WB24 method, and 64% smaller when compared with the WB method. As the f_c reduces, the gap between methods becomes smaller: while for the 3.6 mm/h the $h_{\max,ap}$ is 83 and 76% smaller than $h_{\max,WB24}$, and $h_{\max,WB}$, respectively, for the 0.36 mm/h the reduction is 47 and 44%.

In Figure 6, the h_{\max} and outflow probability for the event-based (WB24 and WB) and AP models were plotted with the outflow frequency obtained with the continuous simulation held on EPA-SWMM. The continuous simulation using SWMM considers evapotranspiration and rainfall-runoff transformation, both neglected for the event-based and AP methods.

For all design methods used in this study and the continuous simulations, hydraulic conductivity was assumed to be constant and equal to f_c . Outflows were represented in EPA-SWMM as discharge from the underdrains placed at a h_{\max} offset. EPA-SWMM efficiency in modeling permeable pavement is broadly reported in the literature, and robustness increases for time steps lower than 1 h (Zhang & Guo 2015b; Randall *et al.* 2020; Arjenaki *et al.* 2021; Parnas *et al.* 2021). As the unsaturated condition of the infiltration process is not represented by EPA-SWMM, the results could overestimate overflows. For a design tool performance evaluation, this error leads to an analysis in favor of safety. A more detailed description of the infiltration processes would increase robustness and could be obtained by solving Richard's equation or comparing results from full-scale experimental settlements (Brunetti *et al.* 2016; Turco *et al.* 2017).

The outflow frequency with EPA-SWMM (R_{SWMM}) was obtained by considering the number of outflows for storm events divided by the number of storm events for each h_{\max} and f_c . For the EPA-SWMM simulation, a contribution area was not considered ($r = 0$). Both event-based methods overestimate the outflow frequency, while the AP approach gave results close to the continuous simulation as the h_{\max} increased. The overestimation for the event-based methods (WB and WB24) is less pronounced as the infiltration capacity of the soil reduces, and the effect of overlapping storm events is more pronounced.

Observing Figure 7, it is noticed that outflow frequency is slightly overestimated with the event-based continuous simulation from Equations (5) and (6) where outflows are considered after each independent storm event (IETD = 4 h), while EPA-SWMM solves the mass conversation equation with a 10-min time step for both runoff-rainfall transformation and routing during wet periods and a 60-min time step for dry periods with the input of the rainfall series with $\Delta t = 10$ min (IETD = 10 min). The outflow frequency overestimation is due not only to the evapotranspiration effect but also to the difference in IETD and rainfall-runoff time steps. The AP method analytical equations (Equations (8) and (9)) were obtained considering the event-based processes described in Equations (5) and (6), which can explain the overestimation when compared with the EPA-SWMM simulation.

Table 7 | Permeable pavement reservoir depth (h_{\max}) with different hydraulic design methodologies

P_R^a (-)	T (years)	$f_c = 3.6 \text{ mm/h } (10^{-6} \text{ m/s})$			$f_c = 1.8 \text{ mm/h } (5 \times 10^{-7} \text{ m/s})$			$f_c = 0.36 \text{ mm/h } (10^{-7} \text{ m/s})$		
		$h_{\max,WB24}$ (mm)	$h_{\max,WB}$ (mm)	$h_{\max,AP}$ (mm)	$h_{\max,WB24}$ (mm)	$h_{\max,WB}$ (mm)	$h_{\max,AP}$ (mm)	$h_{\max,WB24}$ (mm)	$h_{\max,WB}$ (mm)	$h_{\max,AP}$ (mm)
0.50	2	168	106	^b	177	124	0	184	165	23
0.20	5	231	155	20	240	179	35	247	227	75
0.07	15	296	209	55	305	237	70	312	292	165
0.04	25	325	233	75	334	263	90	341	322	225
0.02	50	364	266	95	373	299	115	380	361	285
0.01	100	403	299	115	412	335	130	419	399	345

Note: WB24, water balance with 24 h storm; WB, water balance with critical storm and AP, analytical-probabilistic approach.

^aOutflow probability.

^bWithout a reservoir ($h_{\max} = 0$), the outflow probability was $P = 0.32$ ($T =$ three years).

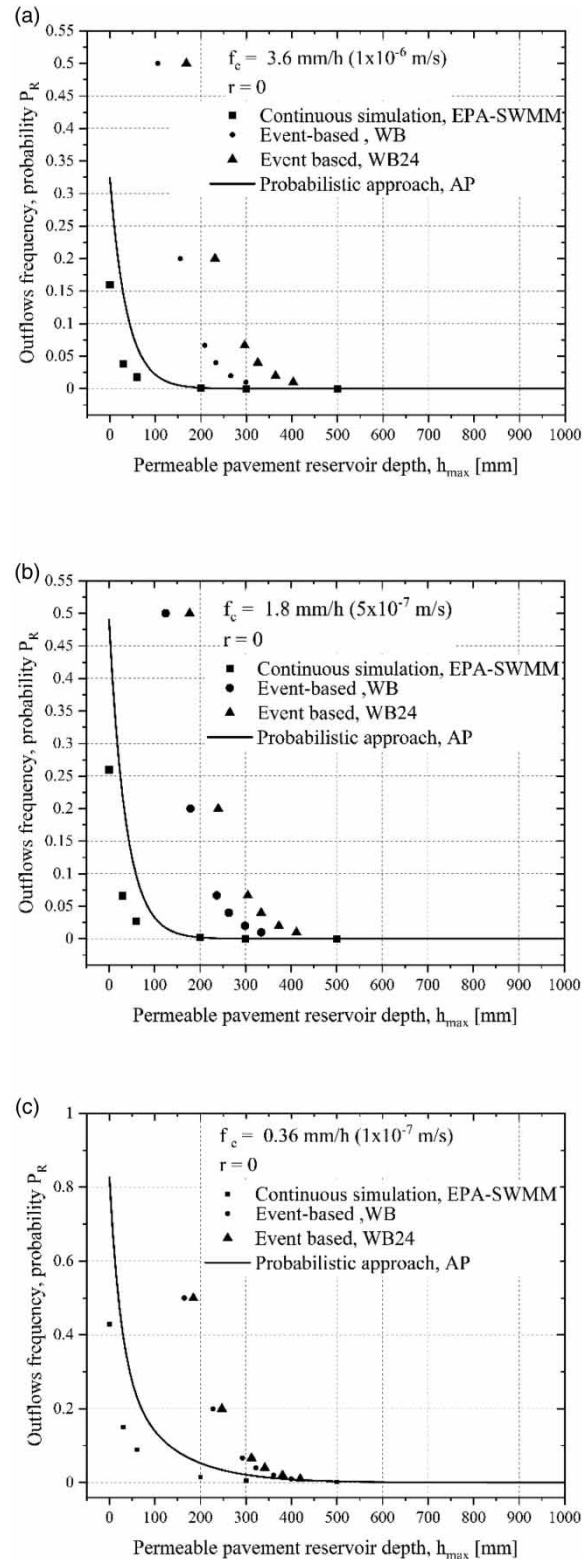


Figure 5 | Maximum water depth (h_{max}) obtained with three design methods (WB24, WB, and AP) for saturated hydraulic conductivity. Return periods (T) of 2, 5, 15, 25, 50, and 100 years. (a) Soil-saturated hydraulic conductivity, $f_c = 3.6 \text{ mm/h}$ ($1 \times 10^{-6} \text{ m/s}$); (b) soil-saturated hydraulic conductivity, $f_c = 1.8 \text{ mm/h}$ ($5 \times 10^{-7} \text{ m/s}$); (c) soil-saturated hydraulic conductivity $f_c = 0.36 \text{ mm/h}$ ($1 \times 10^{-7} \text{ m/s}$).

Table 8 shows for each f_c considered the registered outflows for the continuous simulation with EPA-SWMM (R_{SWMM}), the peak flow, and runoff volume for m^2 for the entire simulated period (10 years). For the simulated period, the $h_{max} = 300 \text{ mm}$ resulted in no outflows for $f_c = 3.6 \text{ mm/h}$ and $f_c = 1.8 \text{ mm/h}$ while for $f_c = 0.36 \text{ mm/h}$

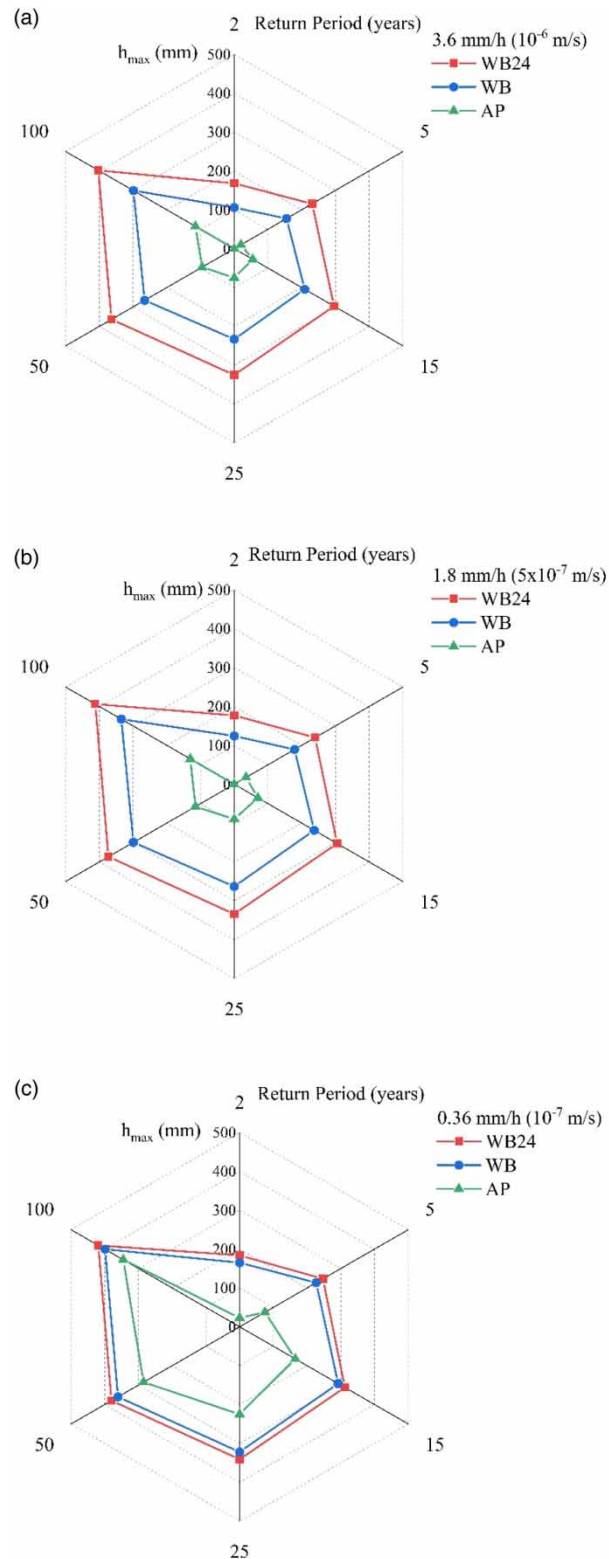


Figure 6 | Event-based methods (WB, WB24) and probabilistic approach (AP) for outflow probability represented as a return period in years for a permeable pavement reservoir depth (h_{\max}). The contribution area was zero ($r=0$). (a) Soil-saturated hydraulic conductivity, $f_c = 3.6 \text{ mm/h}$ ($1 \times 10^{-6} \text{ m/s}$); (b) soil-saturated hydraulic conductivity, $f_c = 1.8 \text{ mm/h}$ ($5 \times 10^{-7} \text{ m/s}$); (c) soil-saturated hydraulic conductivity, $f_c = 0.36 \text{ mm/h}$ ($1 \times 10^{-7} \text{ m/s}$).

a $h_{\max} = 700 \text{ mm}$ led to no outflows. For comparison purposes [Table 8](#) also shows the peak flow (256 L/s) and volume ($2,735,659 \text{ m}^3/\text{m}^2$) without permeable pavement, considering an impermeable surface (98% imperviousness), where the efficiency of the permeable pavement under all scenarios on reducing peak flow and volume is clear.

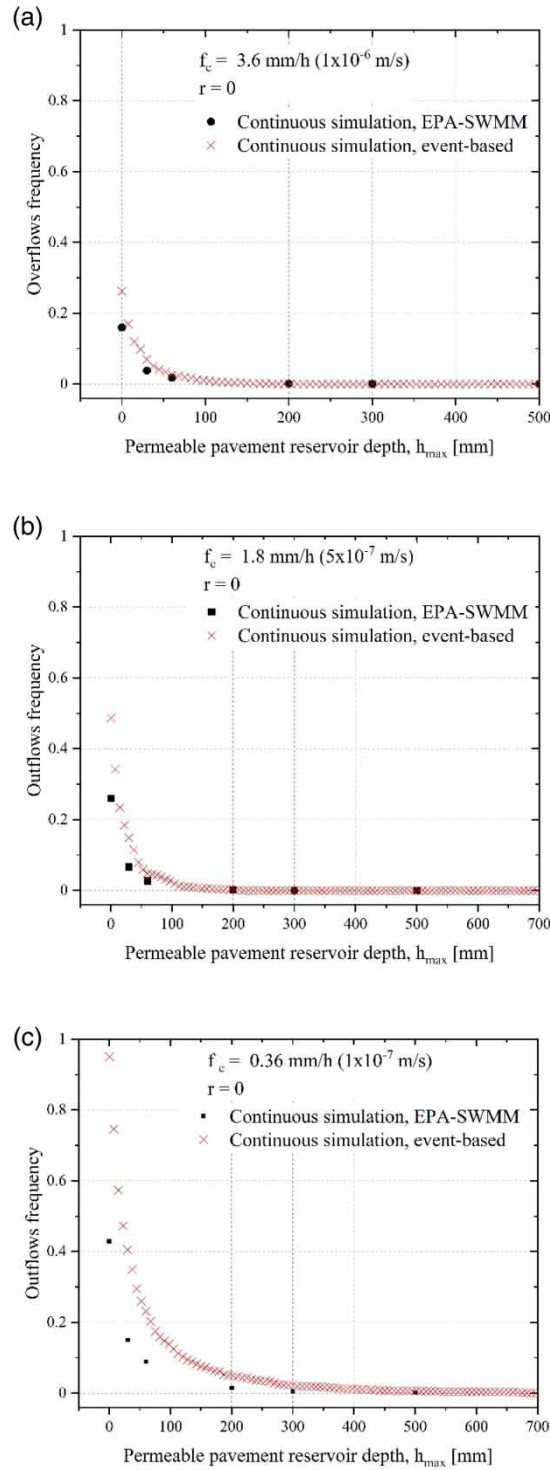


Figure 7 | Event-based and EPA-SWMM continuous simulation for outflow frequency for a permeable pavement h_{\max} reservoir depth. The contribution area was zero ($r = 0$). (a) Soil-saturated hydraulic conductivity, $f_c = 3.6 \text{ mm/h } (1 \times 10^{-6} \text{ m/s})$; (b) soil-saturated hydraulic conductivity, $f_c = 1.8 \text{ mm/h } (5 \times 10^{-7} \text{ m/s})$; (c) soil-saturated hydraulic conductivity, $f_c = 0.36 \text{ mm/h } (1 \times 10^{-7} \text{ m/s})$.

For the h_{\max} simulated in EPA-SWMM, the frequency of outflows (R_{SWMM}) falls below an acceptable performance for stormwater control structures for small catchments, normally designed to manage frequent storm events. For a $T = 50$ years ($P_R = 0.02$), already above what is usually recommended for such structures, the $h_{\max, \text{AP}}$ results on the continuous simulation show an acceptable frequency of outflows, below the expected probability. Smaller h_{\max} was not considered as, for practical reasons, a reservoir depth below 150 mm is not recommended

Table 8 | Outflows, peak flow, and volume for continuous simulation held with EPA-SWMM

f_c (mm/h)	h_{max} (mm)	Reservoir depth (mm)	Outflows ^a (-)	R_{SWMM} (-)	Peak flow ^b (L/s)	Volume ^c (m ³ /m ²)
	Conventional non-permeable pavement (98% imperviousness)					
0.36	0	100	3,356	0.429	0.94	11,615
0.36	30	130	1,178	0.151	1.19	5,896
0.36	60	160	699	0.089	1.15	3,756
0.36	200	300	118	0.015	0.52	917
0.36	300	400	47	0.006	0.52	423
0.36	500	600	14	0.002	0.31	103
1.8	0	100	2,032	0.260	0.93	8,590
1.8	30	130	518	0.066	1.17	3,575
1.8	60	160	212	0.027	0.75	1,827
1.8	200	300	16	0.002	0.27	144
1.8	300	400	2	0.000	0.12	9
1.8	500	600	0	0.000	0	0
3.6	0	100	1,249	0.160	0.93	6,464
3.6	30	130	298	0.038	1.16	2,546
3.6	60	160	139	0.018	0.74	1,286
3.6	200	300	9	0.001	0.26	58
3.6	300	400	0	0.000	0	0
3.6	500	600	0	0.000	0	0

Note: Bold highlights h_{max} without outflows during the simulated period.

^aNumber of outflows, as discharge from the underdrain, considering a total of 7,823 storm events in 10 years.

^bPeak flow for the permeable pavement runoff for the entire simulated period.

^cTotal runoff volume for the entire simulated period for m².

^dPeak flow and volume without permeable pavement.

(Marchioni & Becciu 2015; Swan & Smith s.d.). The $h_{max, WB}$ for $T = 50$ years result in zero outflows for both $f_c = 3.6$ mm/h and $f_c = 1.8$ mm/h when considering the EPA-SWMM continuous simulation, a performance well above the expected probability. For $f_c = 0.36$ mm/h outflows were observed, highlighting the effect of overlapping storm events, where the reservoir was not empty completely after the previous event increasing the outflow probability. With the AP method, the probability of no outflows ($P_R = 0$) was reached for $h_{max, ap} = 975$ mm.

The AP approach has already been used for the permeable pavement with the scope of evaluating the performance (Zhang & Guo 2015a; Guo *et al.* 2018) whereas this research is proposed as a design tool to obtain the reservoir depth h_{max} . The AP model has robustness comparable to continuous simulation, whereas event-based methods showed an overestimation of the probability of outflows. The overestimation between single-storm methods and the AP approach is smaller for low hydraulic conductivity, where the AP considers the effect of concatenated events, which in this case will certainly influence the frequency of outflows. With respect to the results presented, adopting the AP approach to design permeable pavement systems reduces h_{max} with an acceptable performance when considering the usual exceedance probability for small stormwater control structures, leading to saving costs and reducing environmental impacts from construction and raw materials.

4. CONCLUSIONS

The AP model allows for the determination of an analytical equation derived from the rainfall PDF that describes the main hydrological processes in stormwater controls. In this research, the AP was used as a design tool to obtain a permeable pavement reservoir depth, h_{max} , the probability of outflows, translated also as a probability of exceedance occurrence, or simply return period as usual terminology on stormwater management. The AP equation proposed includes the probability of concatenated storm events, a condition especially relevant for low-release controls, as in the case of permeable pavement placed over low-permeability soil.

Results obtained with the AP approach were compared with event-based design methods and with a continuous simulation using EPA-SWMM. The methods presented were applied with a rainfall series and IDF from São Paulo (Brazil) to demonstrate their efficiency compared with traditional methods. The application of the AP model led to a reduction of reservoir depth, h_{\max} with a probability of outflow analogous to continuous simulation. Reducing h_{\max} translates to a reduction in excavation and aggregate volume translating directly into cost and environmental impacts on energy and greenhouse emissions reduction, justifying especially on large-scale developments the adoption of a more robust design method such as AP.

Simple design tools such as the WB24 are straightforward and simple to use and are a good option for preliminary design or for small-scale projects where the cost impact will be limited, and the design is not held by an expert. However, for large-scale projects having a more accurate tool available can lead to substantial advantages in helping the dissemination of permeable pavement systems. The performance of the AP method was assessed through continuous simulation with EPA-SWMM; however, it can overestimate overflows by neglecting the infiltration process for non-saturated conditions. Although the error in this cause is in favor of safety, future developments could compare the method results with detailed modeling of the infiltration process by solving Richard's equation or with full-scale experimental results.

With the increase of temporary storage controls on stormwater management, often mandatory or deeply advisable by local policies and regulations having available several design tools with different levels of complexity on application, input data necessary and robustness can assist developers and designers. Research shows that the probabilistic approach is an effective tool to design stormwater controls that are successfully used on permeable pavement systems, green roofs, trenches, and storage units.

The preliminary results here presented from the application to the case study show a better performance of the AP with respect to simple event-based approaches. Application to more case studies from different climatic contexts and comparison with field measurements will be part of the development of the research to further assess the performance of the AP to improve the design of permeable pavements and stormwater controls with storage.

ACKNOWLEDGEMENTS

This research was funded by Politecnico di Milano. The rainfall series used in this research was supplied by FCTH (Fundação Centro Tecnológico de Hidráulica).

DATA AVAILABILITY STATEMENT

All relevant data are included in the paper or its Supplementary Information.

CONFLICT OF INTEREST

The authors declare there is no conflict.

REFERENCES

- Abdalla, E. M. H., Selseth, I., Muthanna, T. M., Helness, H., Alfredsen, K., Gaarden, T. & Sivertsen, E. 2021 [Hydrological performance of lined permeable pavements in Norway](https://doi.org/10.2166/bgs.2021.009). *Blue-Green Systems* **3** (1), 107–118. <https://doi.org/10.2166/bgs.2021.009>.
- Abdalla, E. M. H., Muthanna, T. M., Alfredsen, K. & Sivertsen, E. 2022 [Towards improving the hydrologic design of permeable pavements](https://doi.org/10.2166/bgs.2022.004). *Blue-Green Systems* **4** (2), 197–212. <https://doi.org/10.2166/bgs.2022.004>.
- Adams, B. J. & Papa, F. 2001 *Urban Stormwater Management Planning with Analytical Probabilistic Models*.
- Adams, B. J., Fraser, H. G., Howard, C. D. D. & Sami Hanafy, M. 1986 [Meteorological data analysis for drainage system design](https://doi.org/10.1061/(ASCE)0733-9372(1986)112:5(827)). *Journal of Environmental Engineering* **112** (5), 827–848. [https://doi.org/10.1061/\(ASCE\)0733-9372\(1986\)112:5\(827\)](https://doi.org/10.1061/(ASCE)0733-9372(1986)112:5(827)).
- Altobelli, M., Cipolla, S. S. & Maglionico, M. 2020 [Combined application of real-time control and green technologies to urban drainage systems](https://doi.org/10.1016/j.watres.2020.115832). *Water* **12** (12), 3432. <https://doi.org/10.1016/j.watres.2020.115832>.
- Alvares, C. A., Stape, J. L., Sentelhas, P. C., de Moraes Gonçalves, J. L. & Sparovek, G. 2013 [Köppen's climate classification map for Brazil](https://doi.org/10.1127/0941-2948/2013/0507). *Meteorologische Zeitschrift* **22**, 711–728. <https://doi.org/10.1127/0941-2948/2013/0507>.
- Andersen, C. T., Foster, I. D. L. & Pratt, C. J. 1999 [The role of urban surfaces \(permeable pavements\) in regulating drainage and evaporation: Development of a laboratory simulation experiment](https://doi.org/10.1002/(SICI)1099-1085(199903)13:4<597::AID-HYP756>3.0.CO;2-Q). *Hydrological Processes* **13** (4), 597–609. [https://doi.org/10.1002/\(SICI\)1099-1085\(199903\)13:4<597::AID-HYP756>3.0.CO;2-Q](https://doi.org/10.1002/(SICI)1099-1085(199903)13:4<597::AID-HYP756>3.0.CO;2-Q).
- Andrés-Valeri, V. C., Marchioni, M., Sañudo-Fontaneda, L. A., Giustozzi, F. & Becciu, G. 2016 [Laboratory assessment of the infiltration capacity reduction in clogged porous mixture surfaces](https://doi.org/10.1016/j.suswat.2016.07.001). *Sustainability* **8** (8), 751. <https://doi.org/10.1016/j.suswat.2016.07.001>.
- Andres-Valeri, V. C., Juli-Gandara, L., Jato-Espino, D. & Rodriguez-Hernandez, J. 2018 [Characterization of the infiltration capacity of porous concrete pavements with low constant head permeability tests](https://doi.org/10.1016/j.watres.2018.03.030). *Water* **10** (4), 480. <https://doi.org/10.1016/j.watres.2018.03.030>.

- Arjenaki, M. O., Sanayei, H. R. Z., Heidarzadeh, H. & Mahabadi, N. A. 2021 [Modeling and investigating the effect of the LID methods on collection network of urban runoff using the SWMM model \(case study: Shahrekord City\)](#). *Modeling Earth Systems and Environment* **7** (1), 1–16. <https://doi.org/10.1007/s40808-020-00870-2>.
- Bacchi, B., Balistocchi, M. & Grossi, G. 2008 [Proposal of a semi-probabilistic approach for storage facility design](#). *Urban Water Journal* **5** (3), 195–208. <https://doi.org/10.1080/15730620801980723>.
- Barbosa, A. E., Fernandes, J. N. & David, L. M. 2012 [Key issues for sustainable urban stormwater management](#). *Water Research* **46** (20), 6787–6798. <https://doi.org/10.1016/j.watres.2012.05.029>.
- Becciu, G. & Raimondi, A. 2012 [Factors affecting the pre-filling probability of water storage tanks](#). 473–484. <https://doi.org/10.2495/WP120411>.
- Becciu, G. & Raimondi, A. 2015 [Probabilistic analysis of the retention time in stormwater detention facilities](#). *Procedia Engineering* **119**, 1299–1307. <https://doi.org/10.1016/j.proeng.2015.08.951>.
- Becciu, G., Raimondi, A. & Dresti, C. 2018 [Semi-probabilistic design of rainwater tanks: A case study in Northern Italy](#). *Urban Water Journal* **15** (3), 192–199. <https://doi.org/10.1080/1573062X.2016.1148177>.
- Beck, H. E., Zimmermann, N. E., McVicar, T. R., Vergopolan, N., Berg, A. & Wood, E. F. 2018 [Present and future Köppen-Geiger climate classification maps at 1-km resolution](#). *Scientific Data* **5** (1), Articolo 1. <https://doi.org/10.1038/sdata.2018.214>.
- Bedient, P. B., Huber, W. C. & Vieux, B. E. 2008 *Hydrology and Floodplain Analysis*, Vol. 816. Prentice Hall Upper Saddle River, NJ.
- Benjamin, J. R. & Cornell, C. A. 1970 *Solutions Manual to Accompany Probability, Statistics, and Decision for Civil Engineers*. McGraw-Hill.
- Brasil, J. B., Guerreiro, M. S., Andrade, E. M. d., de Queiroz Palácio, H. A., Medeiros, P. H. A. & Ribeiro Filho, J. C. 2022 [Minimum rainfall inter-event time to separate rainfall events in a low latitude semi-arid environment](#). *Sustainability* **14** (3), 1721. <https://doi.org/10.3390/su14031721>.
- Brattebo, B. O. & Booth, D. B. 2003 [Long-term stormwater quantity and quality performance of permeable pavement systems](#). *Water Research* **37** (18), 4369–4376.
- Brown, R. A. & Borst, M. 2015 [Quantifying evaporation in a permeable pavement system](#). *Hydrological Processes* **29** (9), 2100–2111. <https://doi.org/10.1002/hyp.10359>.
- Brugin, M., Marchioni, M., Becciu, G., Giustozzi, F., Toraldo, E. & Andrés-Valeri, V. C. 2020 [Clogging potential evaluation of porous mixture surfaces used in permeable pavement systems](#). *European Journal of Environmental and Civil Engineering* **24** (5), 620–630.
- Brunetti, G., Šimůnek, J. & Piro, P. 2016 [A comprehensive numerical analysis of the hydraulic behavior of a permeable pavement](#). *Journal of Hydrology* **540**, 1146–1161. <https://doi.org/10.1016/j.jhydrol.2016.07.030>.
- Cao, S., Diao, Y., Wang, J., Liu, Y., Raimondi, A. & Wang, J. 2023 [KDE-based rainfall event separation and characterization](#). *Water* **15** (3), Articolo 3. <https://doi.org/10.3390/w15030580>.
- Chen, X. & Wang, H. 2022 [Life-cycle assessment and multi-criteria performance evaluation of pervious concrete pavement with fly ash](#). *Resources, Conservation and Recycling* **177**, 105969. <https://doi.org/10.1016/j.resconrec.2021.105969>.
- Chin, R. J., Lai, S. H., Chang, K. B., Jaafar, W. Z. W. & Othman, F. 2016 [Relationship between minimum inter-event time and the number of rainfall events in Peninsular Malaysia](#). *Weather* **71** (9), 213–218. <https://doi.org/10.1002/wea.2766>.
- Coutinho, A. P., Lassabatere, L., Montenegro, S., Antonino, A. C. D., Angulo-Jaramillo, R. & Cabral, J. J. S. P. 2016 [Hydraulic characterization and hydrological behaviour of a pilot permeable pavement in an urban centre, Brazil](#). *Hydrological Processes* **30** (23), 4242–4254. <https://doi.org/10.1002/hyp.10985>.
- Dhakal, K. P. & Chevalier, L. R. 2017 [Managing urban stormwater for urban sustainability: Barriers and policy solutions for green infrastructure application](#). *Journal of Environmental Management* **203**, 171–181.
- Di Chiano, M. G., Marchioni, M., Raimondi, A., Sanfilippo, U. & Becciu, G. 2023 [Probabilistic approach to tank design in rainwater harvesting systems](#). *Hydrology* **10** (3), Articolo 3. <https://doi.org/10.3390/hydrology10030059>.
- Dunkerley, D. 2008 [Identifying individual rain events from pluviograph records: A review with analysis of data from an Australian dryland site](#). *Hydrological Processes* **22** (26), 5024–5036. <https://doi.org/10.1002/hyp.7122>.
- Eagleson, P. S. 1978 [Climate, soil, and vegetation: 2. The distribution of annual precipitation derived from observed storm sequences](#). *Water Resources Research* **14** (5), 713–721. <https://doi.org/10.1029/WR014i005p00713>.
- Elizondo-Martínez, E. J., Andrés-Valeri, V. C., Jato-Espino, D. & Rodríguez-Hernández, J. 2020 [Review of porous concrete as multifunctional and sustainable pavement](#). *Journal of Building Engineering* **27**, 100967.
- Elizondo-Martínez, E. J., Andrés-Valeri, V. C., Juli-Gándara, L. & Rodríguez-Hernández, J. 2022 [Multi-criteria optimum mixture design of porous concrete pavement surface layers](#). *International Journal of Pavement Engineering* **23** (3), 745–754.
- Elliott, A. H. & Trowsdale, S. A. 2007 [A review of models for low impact urban stormwater drainage](#). *Environmental Modelling & Software* **22** (3), 394–405.
- Feki, M., Ravazzani, G., Ceppi, A., Milleo, G. & Mancini, M. 2018 [Impact of infiltration process modeling on soil water content simulations for irrigation management](#). *Water* **10** (7), Articolo 7. <https://doi.org/10.3390/w10070850>.
- Feki, M., Ravazzani, G., Barontini, S., Ceppi, A. & Mancini, M. 2020 [A comparative assessment of the estimates of the saturated hydraulic conductivity of two anthropogenic soils and their impact on hydrological model simulations](#). *Soil and Water Research* **15** (3), 135–147. <https://doi.org/10.17221/33/2019-SWR>.
- Freitas, E. d. S., Coelho, V. H. R., Xuan, Y., Melo, D. d. C. D., Gadelha, A. N., Santos, E. A., Galvão, C. d. O., Ramos Filho, G. M., Barbosa, L. R., Huffman, G. J., Petersen, W. A. & Almeida, C. d. N. 2020 [The performance of the IMERG satellite-based product in identifying sub-daily rainfall events and their properties](#). *Journal of Hydrology* **589**, 125128. <https://doi.org/10.1016/j.jhydrol.2020.125128>.

- Gobatti, L. & Leite, B. C. C. 2022 Vegetated roofs rainwater management experimental research in Brazil: A georeferenced exhaustive review of a continental-size country. *Cleaner Production Letters* **100013**.
- Gobatti, L., Martins, J. R. S., Pereira, M. C. S. & Leite, B. C. C. 2022 Real-time sensing and low-cost experimental setup for water quantity investigation in nature-based solutions. *Blue-Green Systems* **4** (2), 75–88.
- Goulden, S., Portman, M. E., Carmon, N. & Alon-Mozes, T. 2018 From conventional drainage to sustainable stormwater management: Beyond the technical challenges. *Journal of Environmental Management* **219**, 37–45.
- Guo, Y. & Adams, B. J. 1999 An analytical probabilistic approach to sizing flood control detention facilities. *Water Resources Research* **35** (8), 2457–2468. <https://doi.org/10.1029/1999WR900125>.
- Guo, Y., Zhang, S. & Liu, S. 2014 Runoff reduction capabilities and irrigation requirements of green roofs. *Water Resources Management* **28** (5), 1363–1378. <https://doi.org/10.1007/s11269-014-0555-9>.
- Guo, R., Guo, Y. & Wang, J. 2018 Stormwater capture and antecedent moisture characteristics of permeable pavements. *Hydrological Processes* **32** (17), 2708–2720. <https://doi.org/10.1002/hyp.13213>.
- Guo, Y., Asce, M. & Baetz, B. W. s.d. Sizing of Rainwater Storage Units for Green Building Applications. <https://doi.org/10.1061/ASCE1084-0699200712:2197>.
- Hassini, S. & Guo, Y. 2022 Analytical derivation of urban runoff-volume frequency models. *Journal of Sustainable Water in the Built Environment* **8** (1), 04021022. <https://doi.org/10.1061/JSWBAY.0000968>.
- Ignaccolo, M. & De Michele, C. 2010 A point based Eulerian definition of rain event based on statistical properties of inter drop time intervals: An application to Chilbolton data. *Advances in Water Resources* **33** (8), 933–941. <https://doi.org/10.1016/j.advwatres.2010.04.002>.
- Iqbal, A., Rahman, M. M. & Beecham, S. 2022 Permeable pavements for flood control in Australia: Spatial analysis of pavement design considering rainfall and soil data. *Sustainability* **14** (9), Articolo 9. <https://doi.org/10.3390/su14094970>.
- Kia, A., Wong, H. S. & Cheeseman, C. R. 2017 Clogging in permeable concrete: A review. *Journal of Environmental Management* **193**, 221–233.
- Kia, A., Delens, J. M., Wong, H. S. & Cheeseman, C. R. 2021 Structural and hydrological design of permeable concrete pavements. *Case Studies in Construction Materials* **15**, e00564. <https://doi.org/10.1016/j.cscm.2021.e00564>.
- Kim, J. Y. & Sansalone, J. J. 2008 Event-based size distributions of particulate matter transported during urban rainfall-runoff events. *Water Research* **42** (10–11), 2756–2768.
- Kuang, X. & Fu, Y. 2013 Coupled infiltration and filtration behaviours of concrete porous pavement for stormwater management. *Hydrological Processes* **27** (4), 532–540. <https://doi.org/10.1002/hyp.9279>.
- Langeveld, J. G., Cherqui, F., Tschekner-Gratl, F., Muthanna, T. M., Juarez, M. F.-D., Leitão, J. P., Roghani, B., Kerres, K., do Céu Almeida, M., Wery, C. & Rulleau, B. 2022 Asset management for blue-green infrastructures: A scoping review. *Blue-Green Systems* **4** (2), 272–290. <https://doi.org/10.2166/bgs.2022.019>.
- Lee, E. H. & Kim, J. H. 2018 Development of new inter-event time definition technique in urban areas. *KSCE Journal of Civil Engineering* **22** (10), 3764–3771. <https://doi.org/10.1007/s12205-018-1120-5>.
- Lieberherr, E. & Green, O. O. 2018 Green infrastructure through citizen stormwater management: Policy instruments, participation and engagement. *Sustainability* **10** (6), 2099.
- Liu, J., Li, H., Wang, Y. & Zhang, H. 2020 Integrated life cycle assessment of permeable pavement: Model development and case study. *Transportation Research Part D: Transport and Environment* **85**, 102381. <https://doi.org/10.1016/j.trd.2020.102381>.
- Lobo Marchioni, M., Raimondi, A., Sanfilippo, U., Sansalone, J., Mambretti, S. & Becciu, G. 2021 Modeling of particulate matter fate on urban highway stormwater control systems. *International Journal of Computational Methods and Experimental Measurements* **9** (1), 1–13.
- Lobo Marchioni, M., Di Chiano, M. G., Raimondi, A., Dresti, C., Sanfilippo, U., Sansalone, J. & Becciu, G. 2022 Permeable pavements efficiency under clogging and pollutants load removal. In: *Innovative Water Management in a Changing Climate*. Abstract book, IAHR Europe Congress 2022.
- Lucke, T. & Nichols, P. W. 2015 The pollution removal and stormwater reduction performance of street-side bioretention basins after ten years in operation. *Science of the Total Environment* **536**, 784–792.
- Marchioni, M. & Becciu, G. 2015 Experimental results on permeable pavements in urban areas: A synthetic review. *International Journal of Sustainable Development and Planning* **10**, 6. <https://doi.org/10.2495/SDP-V10-N6-806-817>.
- Marchioni, M. & Becciu, G. 2018 Infiltration-exfiltration system for stormwater runoff volume and peak attenuation. *International Journal of Safety and Security Engineering* **8** (4), 473–483.
- Medina-Cobo, M. T., García-Marín, A. P., Estévez, J. & Ayuso-Muñoz, J. L. 2016 The identification of an appropriate minimum inter-event time (MIT) based on multifractal characterization of rainfall data series: minimum inter-event time (MIT) and scale invariance of rainfall data. *Hydrological Processes* **30** (19), 3507–3517. <https://doi.org/10.1002/hyp.10875>.
- Molina-Sanchis, I., Lázaro, R., Arnau-Rosalén, E. & Calvo-Cases, A. 2016 Rainfall timing and runoff: The influence of the criterion for rain event separation. *Journal of Hydrology and Hydromechanics* **64** (3), 226–236. <https://doi.org/10.1515/johh-2016-0024>.
- Morgenroth, J., Buchan, G. & Scharenbroch, B. C. 2015 Belowground effects of porous pavements – soil moisture and chemical properties. *Ecological Engineering* **51**, 221–228.
- Mullaney, J. & Lucke, T. 2014 Practical review of pervious pavement designs. *CLEAN–Soil, Air, Water* **42** (2), 111–124.
- Nemirovsky, E. M., Welker, A. L. & Lee, R. 2013 Quantifying evaporation from pervious concrete systems: Methodology and hydrologic perspective. *Journal of Irrigation and Drainage Engineering* **139** (4), 271–277. [https://doi.org/10.1061/\(ASCE\)IR.1943-4774.0000541](https://doi.org/10.1061/(ASCE)IR.1943-4774.0000541).

- Palla, A. & Gnecco, I. 2015 Hydrologic modeling of low impact development systems at the urban catchment scale. *Journal of Hydrology* **528**, 361–368.
- Palla, A., Gnecco, I., Carbone, M., Garofalo, G., Lanza, L. G. & Piro, P. 2015 Influence of stratigraphy and slope on the drainage capacity of permeable pavements: Laboratory results. *Urban Water Journal* **12** (5), 394–403.
- Parnas, F. E. Á., Abdalla, E. M. H. & Muthanna, T. M. 2021 Evaluating three commonly used infiltration methods for permeable surfaces in urban areas using the SWMM and STORM. *Hydrology Research* **52** (1), 160–175. <https://doi.org/10.2166/nh.2021.048>.
- Raimondi, A. & Becciu, G. 2014a Probabilistic design of multi-use rainwater tanks. *Procedia Engineering* **70**, 1391–1400. <https://doi.org/10.1016/j.proeng.2014.02.154>.
- Raimondi, A. & Becciu, G. 2014b Probabilistic modeling of rainwater tanks. *Procedia Engineering* **89**, 1493–1499. <https://doi.org/10.1016/j.proeng.2014.11.437>.
- Raimondi, A. & Becciu, G. 2015 On pre-filling probability of flood control detention facilities. *Urban Water Journal* **12** (4), 344–351. <https://doi.org/10.1080/1573062X.2014.901398>.
- Raimondi, A., Marchioni, M., Sanfilippo, U. & Becciu, G. 2021 Vegetation survival in green roofs without irrigation. *Water (Switzerland)* **13** (2). <https://doi.org/10.3390/w13020136>.
- Raimondi, A., Di Chiano, M. G., Marchioni, M., Sanfilippo, U. & Becciu, G. 2022 Probabilistic modeling of sustainable urban drainage systems. *Urban Ecosystems*. <https://doi.org/10.1007/s11252-022-01299-4>.
- Raimondi, A., Sanfilippo, U., Marchioni, M., Di Chiano, M. G. & Becciu, G. 2023 Influence of climatic parameters on the probabilistic design of green roofs. *Science of The Total Environment* **865**, 161291. <https://doi.org/10.1016/j.scitotenv.2022.161291>.
- Randall, M., Støvring, J., Henrichs, M. & Bergen Jensen, M. 2020 Comparison of SWMM evaporation and discharge to in-field observations from lined permeable pavements. *Urban Water Journal* 491–502. <https://doi.org/10.1080/1573062X.2020.1776737>.
- Ranieri, V., Colonna, P., Sansalone, J. J. & Sciddurlo, A. 2012 Measurement of hydraulic conductivity in porous mixes. *Transportation Research Record* **2295**, 1–10. <https://doi.org/10.3141/2295-01>.
- Ravazzani, G., Caloiero, T., Feki, M. & Pellicone, G. 2018 Impact of infiltration process modeling on runoff simulations: The Bonis River Basin. *Proceedings* **2** (11), Articolo 11. <https://doi.org/10.3390/proceedings2110638>.
- Razzaghmanesh, M. & Borst, M. 2018 Investigation clogging dynamic of permeable pavement systems using embedded sensors. *Journal of Hydrology* **557**, 887–896.
- Riva, M., Mambretti, S., Chaynikov, S., Ackerer, P., Fasanwon, O. & Guadagnini, A. 2013 New general analytical solution for infiltration structures design. *Journal of Hydraulic Engineering* **139** (6), 637–644. [https://doi.org/10.1061/\(ASCE\)HY.1943-7900.0000718](https://doi.org/10.1061/(ASCE)HY.1943-7900.0000718).
- Sansalone, J., Kuang, X., Ying, G. & Ranieri, V. 2012 Filtration and clogging of permeable pavement loaded by urban drainage. *Water Research* **46** (20), 6763–6774. <https://doi.org/10.1016/j.watres.2011.10.018>.
- Scholz, M. & Grabowiecki, P. 2007 Review of permeable pavement systems. *Building and Environment* **42** (11), 3830–3836.
- Swan, D. J. & Smith, D. R. s.d. Development of design system for permeable interlocking concrete pavement. In: *Green Streets and Highways 2010*, pp. 314–322. [https://doi.org/10.1061/41148\(389\)26](https://doi.org/10.1061/41148(389)26).
- Terzaghi, K., Peck, R. B. & Mesri, G. 1996 *Soil Mechanics in Engineering Practice*. John Wiley & Sons.
- Tirpak, R. A., Winston, R. J., Feliciano, M., Dorsey, J. D. & Epps, T. H. 2021 Impacts of permeable interlocking concrete pavement on the runoff hydrograph: Volume reduction, peak flow mitigation, and extension of lag times. *Hydrological Processes* **35** (4), e14167. <https://doi.org/10.1002/hyp.14167>.
- Turco, M., Kodešová, R., Brunetti, G., Nikodem, A., Fér, M. & Piro, P. 2017 Unsaturated hydraulic behaviour of a permeable pavement: Laboratory investigation and numerical analysis by using the HYDRUS-2D model. *Journal of Hydrology* **554**, 780–791. <https://doi.org/10.1016/j.jhydrol.2017.10.005>.
- Turco, M., Brunetti, G., Porti, M., Grossi, G., Maiolo, M. & Piro, P. 2019 Metals potential removal efficiency of permeable pavement. In: *New Trends in Urban Drainage Modelling: UDM 2018 11*. Springer International Publishing, pp. 163–168.
- Turco, M., Brunetti, G., Palermo, S. A., Capano, G., Grossi, G., Maiolo, M. & Piro, P. 2020 On the environmental benefits of a permeable pavement: Metals potential removal efficiency and life cycle assessment. *Urban Water Journal* **17** (7), 619–627.
- UN DESA 2019 *World Urbanization Prospects: The 2018 Revision (st/esa/ser. A/420)*. United Nations, New York, NY, USA.
- Winston, R. J., Davidson-Bennett, K. M., Buccier, K. M. & Hunt, W. F. 2016 Seasonal variability in stormwater quality treatment of permeable pavements situated over heavy clay and in a cold climate. *Water, Air, and Soil Pollution* **227** (5). <https://doi.org/10.1007/s11270-016-2839-6>.
- Winston, R. J., Arend, K., Dorsey, J. D. & Hunt, W. F. 2020 Water quality performance of a permeable pavement and stormwater harvesting treatment train stormwater control measure. *Blue-Green Systems* **2** (1), 91–111. <https://doi.org/10.2166/bgs.2020.914>.
- Woods-Ballard, B., Kellagher, R., Martin, P., Jefferies, C., Bray, R. & Shaffer, P. 2007 *The SUDS Manual*, Vol. 697. Ciria, London.
- Xu, T., Jia, H., Wang, Z., Mao, X. & Xu, C. 2017 SWMM-based methodology for block-scale LID-BMPs planning based on site-scale multi-objective optimization: A case study in Tianjin. *Frontiers of Environmental Science & Engineering* **11** (4), 1. <https://doi.org/10.1007/s11783-017-0934-6>.
- Yiping Guo, B. s.d. *Hydrologic Design of Urban Flood Control Detention Ponds*.
- Zhang, K. & Chui, T. F. M. 2020 Design measures to mitigate the impact of shallow groundwater on hydrologic performance of permeable pavements. *Hydrological Processes* **34** (25), 5146–5166. <https://doi.org/10.1002/hyp.13935>.

- Zhang, S. & Guo, Y. 2015a Analytical equation for estimating the stormwater capture efficiency of permeable pavement systems. *Journal of Irrigation and Drainage Engineering* **141** (4), 06014004. [https://doi.org/10.1061/\(asce\)ir.1943-4774.0000810](https://doi.org/10.1061/(asce)ir.1943-4774.0000810).
- Zhang, S. & Guo, Y. 2015b SWMM simulation of the storm water volume control performance of permeable pavement systems. *Journal of Hydrologic Engineering* **20** (8), 06014010. [https://doi.org/10.1061/\(asce\)he.1943-5584.0001092](https://doi.org/10.1061/(asce)he.1943-5584.0001092).

First received 30 January 2023; accepted in revised form 5 December 2023. Available online 14 December 2023